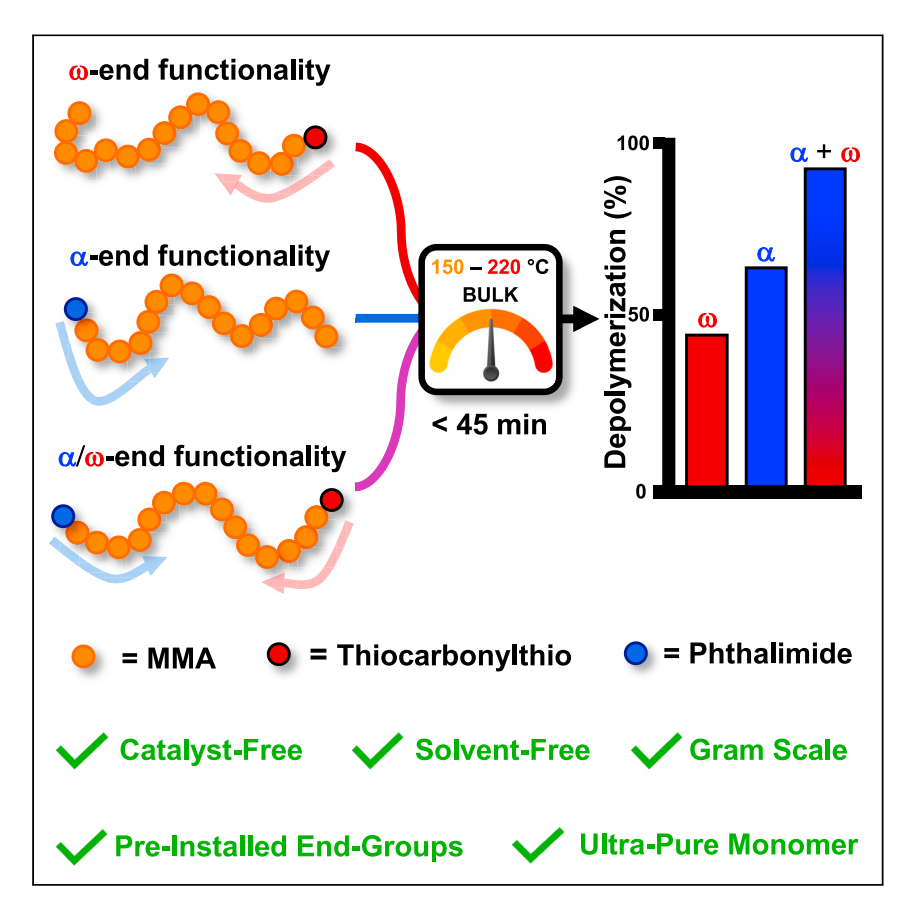




Article

Bulk depolymerization of poly(methyl methacrylate) via chain-end initiation for catalyst-free reversion to monomer



We present the bulk depolymerization of poly(methyl methacrylate) (PMMA) at significantly lower temperatures than previously reported methods through the incorporation of thermolytically labile end-groups via reversible-deactivation radical polymerization (RDRP). This depolymerization methodology allows catalyst- and solvent-free reversion to monomer on a multigram scale at temperatures up to 250°C lower than current industrial methods.

James B. Young, Rhys W. Hughes, Ariana M. Tamura, Laura S. Bailey, Kevin A. Stewart, Brent S. Sumerlin

sumerlin@chem.ufl.edu

Highlights

Catalyst- and solvent-free chemical recycling of PMMA to MMA

Activation of labile chain ends at elevated temperatures yields >90% monomer recovery

Method applies for polymers up to ultrahigh molecular weight

Selective depolymerization skews molecular weight distributions of polymer blends





Young et al., Chem 9, 1–14 September 14, 2023 © 2023 Elsevier Inc. https://doi.org/10.1016/j.chempr.2023.07.004

Chem



Article

Bulk depolymerization of poly(methyl methacrylate) via chain-end initiation for catalyst-free reversion to monomer

James B. Young,^{1,2} Rhys W. Hughes,^{1,2} Ariana M. Tamura,¹ Laura S. Bailey,¹ Kevin A. Stewart,¹ and Brent S. Sumerlin^{1,3,*}

SUMMARY

We present the bulk depolymerization of poly(methyl methacrylate) (PMMA) at significantly lower temperatures than previously reported methods through the incorporation of thermolytically labile end-groups via reversible-deactivation radical polymerization (RDRP). The combination of $\alpha\text{-end}$ N-hydroxyphthalimide esters and $\omega\text{-end}$ trithiocarbonates allows for near-quantitative depolymerization of PMMA in the bulk, with >90% methyl methacrylate (MMA) recovery for subsequent repolymerization. This depolymerization methodology enables catalyst- and solvent-free reversion to monomer on a multigram scale at temperatures up to 250°C lower than current industrial methods. These reactions are performed in an efficient and high-yielding manner, establishing a viable route to depolymerize PMMA on large scales.

INTRODUCTION

As the demand for plastics continues to rise, a concomitant increase in plastic waste has been observed. In the United States, less than 10% of plastic waste is recycled; therefore, new recycling strategies have become imperative to reduce the negative impact on the environment.²⁻⁴ Current industrial efforts to recycle polymers are generally directed toward thermomechanical recycling, which typically yields lower-quality materials with reduced mechanical properties. 1,5,6 Another promising means of recycling plastic waste involves chemical recycling, a method that can recycle or upcycle polymeric materials via chemical stimuli to degrade polymers to original or higher value materials. ⁷ This method is particularly appealing because the recovered starting material can be re-polymerized to create a variety of polymeric materials with desired mechanical properties. Poly(ethylene terephthalate) (PET), for example, can be chemically recycled by hydrolysis, alcoholysis, or aminolysis of the backbone ester bond. 8,9 The resulting compounds can then be used to regenerate similar, if not identical, polymeric materials. In this case, chemical recycling methods of PET rely on the reactivity of ester functional groups within the polymer backbone.

Polymers synthesized by chain-growth polymerization of vinyl monomers are desirable due to the robustness imparted by their all-carbon backbones; however, the stability of carbon-carbon bonds renders the polymers exceptionally stable and difficult to revert to monomer, ultimately making chemical recycling prohibitively difficult. Methods to degrade vinyl-based polymers have centered around the incorporation of a monomer that introduces heteroatoms to facilitate degradation. ^{10–14} This has been achieved through the radical ring opening of cyclic acetals or

THE BIGGER PICTURE

This work addresses challenges of waste recyclability in response to the call to action proposed in the industry, innovation, and infrastructure section of the United Nations' Sustainable Global Goal Initiatives. The mass production of commodity plastics has outpaced the development of waste remediation of these products, creating an imbalance within production and waste life cycles. We illustrate how polymers prepared via reversibledeactivation radical polymerization (RDRP) can be thermally triggered to depolymerize back to monomer, with the recovered monomer being amenable to repolymerization to generate virgin polymer. This depolymerization strategy may further incentivize the translation of RDRP techniques for industrial polymer synthesis. In addition to current commodity plastic production, emerging fields such as 3D printing and lithography are positioned to adopt recyclable materials into their production methods to close the gap in life cycle circularity of polymer materials.





thiolactones to incorporate degradable linkages in an otherwise all-carbon backbone. $^{14-16}$ Other reports include the incorporation of monomers that are capable of generating backbone radicals to induce degradation through β -cleavage. $^{17-20}$ Recent methods have included the statistical incorporation of phthalimide (Phth) methacrylate/acrylate monomers capable of accepting an electron from a photocatalyst to initiate a cascade reaction that liberates $\rm CO_2$ to induce backbone degradation. 20,21 Although the aforementioned reports involve a side-chain trigger to efficiently cleave carbon–carbon backbone polymers, depolymerization from chain ends has emerged as an appealing approach to address the chemical recyclability of these all-carbon backbone polymers. 22

Poly(methyl methacrylate) (PMMA) is a polymer with an all-carbon backbone produced via chain-growth polymerization. PMMA is a commercial thermoplastic with wide applications as a glass substitute in aircraft, automotive, and construction industries. The production of PMMA currently resides at >4 million tons per year, with usage expected to reach nearly 6 million tons by 2027.²³ The increase in industrial use of PMMA can be attributed to its high mechanical strength and low density compared to glass; however, less than 10% of PMMA is recycled annually. 23 Current methods of depolymerizing PMMA are achieved at high temperatures, ranging from 375°C to 500°C, with monomer collected via a distillation process. However, the recovered monomer is generally only achieved with limited purity. The quantity of MMA recovered is also highly dependent on depolymerization methodology.²⁴ To increase efficiency and monomer purity, high dilution can be used to reduce the ceiling temperature (T_c) of PMMA. This has been achieved with polymers synthesized via reversible addition-fragmentation chain transfer (RAFT) polymerization and atom transfer radical polymerization (ATRP). Although RAFT polymerization and ATRP are normally used to synthesize polymers with controlled molecular weights, low dispersities, and well-defined architectures, recent reports have shown that activation of the chain ends inherent to these polymerization methods at elevated temperatures can trigger depolymerization.^{25–35}

Initial reports by Gramlich and Ouchi demonstrated that the use of labile bonds on the chain ends of PMMA synthesized by RAFT polymerization and ATRP could be used to induce depolymerization through C-S cleavage or halide abstraction. 36,37 More recently, Anastasaki demonstrated that terminal thiocarbonylthio chain ends could yield near-quantitative solution depolymerization under highly dilute conditions by exploiting chain-end C-S bond homolysis at temperatures as low as 120°C.³⁸ Our group demonstrated that depolymerization could be dramatically accelerated, at even lower temperatures (e.g., 100°C), by increasing C-S bond cleavage via photolysis. We also established that the $T_{\rm c}$ of PMMA in dioxane at 5 mM of repeat units resides near 85°C.³⁹ Anastasaki also demonstrated that light could be used to accelerate depolymerization by utilizing an excess of eosin Y via a single electron transfer (SET) process to enhance the rate of terminal bond photolysis.⁴⁰ In another study, Matyjaszewski reported that polymethacrylate polymers synthesized via ATRP can also be depolymerized by leveraging the labile carbonhalogen bond on the polymer chain. Activation of the halogen chain end could be achieved with various copper halide salts, and more concentrated polymer solutions (0.7 M in monomer units) could be employed by increasing the temperature (>170°C) to selectively distill monomer. 41-43 Although the goal of increasing depolymerization efficiency of PMMA has been achieved, the requirements of high dilution and/or the necessity for catalysts may be prohibitory for widespread adoption of reversible-deactivation radical polymerization (RDRP) synthetic methodologies for enabling reversion to high-purity monomer. Block copolymer lithography, in

¹George & Josephine Butler Polymer Research Laboratory, Department of Chemistry, Center for Macromolecular Science & Engineering, University of Florida, Gainesville, FL 32611, USA

²These authors contributed equally

³Lead contact

^{*}Correspondence: sumerlin@chem.ufl.edu https://doi.org/10.1016/j.chempr.2023.07.004

Please cite this article in press as: Young et al., Bulk depolymerization of poly(methyl methacrylate) via chain-end initiation for catalyst-free reversion to monomer, Chem (2023), https://doi.org/10.1016/j.chempr.2023.07.004





addition to increasing material recyclability, is also an appealing potential application in which microphase-separated PMMA regions can be selectively depolymerized to achieve nanopatterned materials.⁴⁴

Reducing, or altogether removing, solvents and catalysts required to reduce the $T_{\rm c}$ of PMMA may further simplify industrial-scale and commercially relevant depolymerizations. Bulk thermal-initiated depolymerization of PMMA usually requires temperatures greater than 375°C and produces a variety of undesirable byproducts that requires further purification of the resulting monomer. Herein, we demonstrate new synthetic approaches to generate PMMA amenable to efficient reversion to MMA by capitalizing on labile chain ends. This approach can be performed on the gram scale without catalyst or solvent. The depolymerization of PMMA prepared by these RDRP techniques can achieve up to 92% reversion to monomer at temperatures 250°C lower than those currently applied on an industrial scale. Key to our approach is the selection of chain-end functional groups that generate terminal radicals above the boiling point of MMA, thus favoring reversion to monomer under non-equilibrium conditions. 45,46

RESULTS AND DISCUSSION

Our pursuit to find chain ends capable of achieving high degrees of depolymerization began by exploring various ω-end thiocarbonylthio functional groups on PMMA prepared via RAFT polymerization (Figure 1A). Specifically, PMMA was prepared by RAFT polymerization with 2-cyanoprop-2-yl dithiobenzoate (PMMA-DTB-H, kg/mol), cyanopropyl-2-yl(4-methoxy) dithiobenzoate (PMMA-DTB-OMe, 5.9 kg/mol), 2-cyanopropyl-2-yl(4-cyano) dithiobenzoate (PMMA-DTB-CN, 5.5 kg/mol), 2-cyanopropan-2-yl N-methyl-N-(pyridin-4-yl)carbamodithioate (PMMA-DTC, 8.1 kg/ mol), and 4-cyano-4-[(dodecylsulfanylthiocarbonyl) sulfanyl] pentanoic acid (PMMA-TTC, 5.3 kg/mol) (Figures 1B and 2). Molecular weights were maintained within ± 1.5 kg/mol to reduce the effects of chain length on the extent of depolymerization. The thermal stability of the RAFT polymer end-groups was then investigated via thermogravimetric analysis (TGA) to determine the onset temperature of depolymerization, which we defined as the temperature at which 95% of the mass remains (T_{95}) (Table S1). Although the temperature for the onset of depolymerization depended on heating rate, lower ramp rates of 5°C/min-10°C/min were found to have the most repeatable onset temperatures of depolymerization (Figure S1). It was observed that the T_{95} for functionalized PMMA ranged from 148°C for PMMA-TTC to 186°C for PMMA-DTB-OMe. PMMA without the RAFT-derived end-groups (PMMA-H) was considerably more stable and did not degrade until temperatures near 376°C (Table S1). Notably, the highest extent of depolymerization was observed with the PMMA-TTC, which reached 42% mass loss until a plateau was observed in the TGA trace. By contrast, the PMMA-DTC achieved 28% depolymerization, whereas the dithiobenzoyl-terminated polymers (PMMA-DTB-H, -CN, -OMe) only reached 4%-7% depolymerization before an observed plateau in the TGA trace (Figure 2). When investigating the reduced extent of depolymerization for the PMMA-DTB samples, ¹H nuclear magnetic resonance (NMR) spectroscopy provided evidence of a predominant side reaction that competed with depolymerization. The major byproducts after thermal treatment were determined to be alkene-terminated PMMA, attributed to the Chugaev-elimination pathway that can occur with thiocarbonylthio functional groups at elevated temperatures (Figures S2 and S3). 47-50 Interestingly, this terminal alkene group enabled a second onset of depolymerization to occur near 310°C (Figure S4). These results agree with previous TGA data reported by Kudryavtsev et al. in which trithiocarbonate-terminated PMMA also demonstrated a higher degree of depolymerization relative to DTB-terminated PMMA.⁵¹





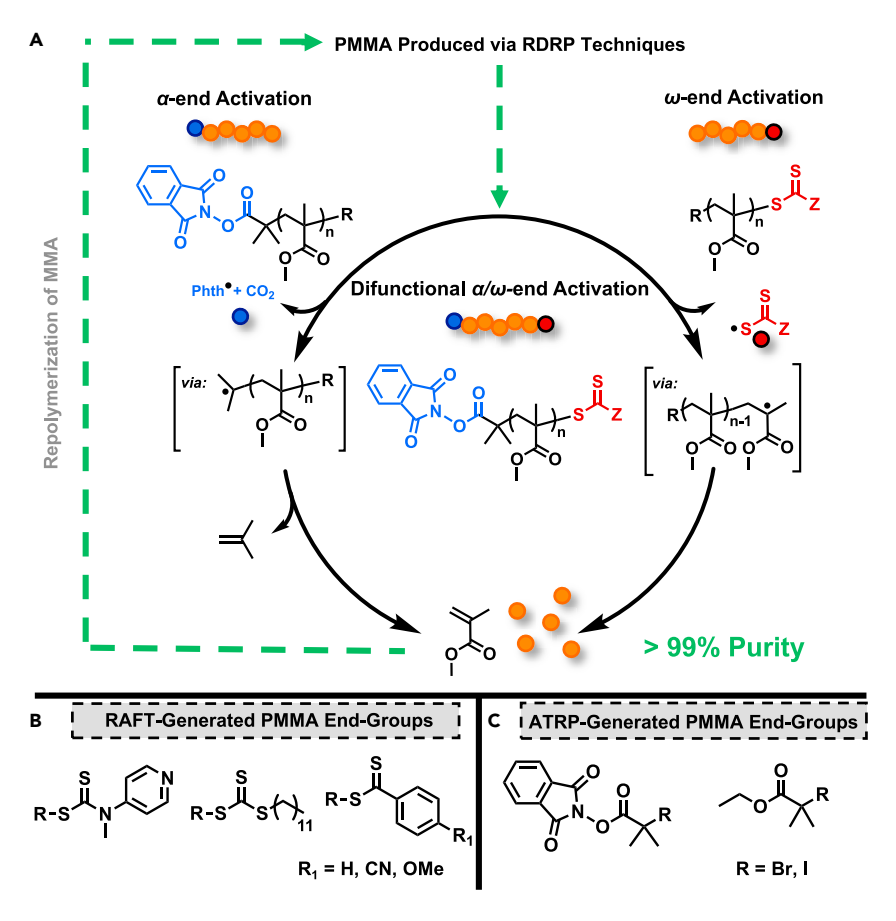


Figure 1. Chemical recycling of PMMA to MMA utilizing labile end-groups (A) Initiation of depolymerization from α -chain ends, ω -chain ends, or a combination of the two. (B and C) This strategy can be applied to polymers derived from (B) reversible addition-fragmentation chain transfer (RAFT) polymerization and (C) atom transfer radical polymerization (ATRP).

In addition to RAFT polymerization, ATRP is one of the most widely used RDRP techniques and generally leads to polymers that are white or colorless, a potential advantage over the yellow- or pink-colored thiocarbonylthio moieties that remain in RAFTgenerated polymers. 52-55 A variety of ATRP-derived chain ends were explored to examine the thermolytic capacity for depolymerization (Figure 1C). Ethyl α -bromo isobuturate (EBIB), a commonly used ATRP initiator, was used to polymerize MMA by supplemental activator and reducing agent (SARA) ATRP.⁵⁶ Thermal treatment of the synthesized PMMA-Br exhibited an onset of depolymerization at 285°C, but only \sim 12% depolymerization was observed (Figure 3). PMMA-Br subsequently underwent treatment with sodium iodide via the Finkelstein reaction to substitute the terminal bromine with iodine. Although a lower onset temperature of depolymerization was observed at 272°C, the extent of depolymerization was only slightly increased to 14%. Due to the lack of efficient depolymerization achieved through thermolysis of the ω -halogen chain ends, we turned our attention to synthesizing PMMA with labile bonds on their α-chain ends. This was achieved by preparing an ATRP initiator containing an N-hydroxy Phth ester. Subsequent polymerization of MMA by SARA ATRP provided the desired polymer (Phth-PMMA-Br) with controlled molecular weight and low dispersity (Figure S5). Analysis of the Phth-PMMA-Br by TGA showed up to 65% depolymerization, with the T_{95} occurring near 220°C





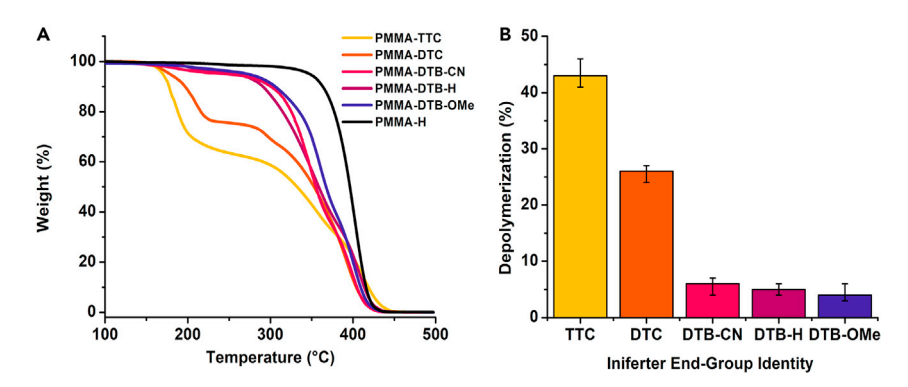


Figure 2. Extent of PMMA depolymerization utilizing RAFT end-groups

(A) Thermogravimetric analysis (TGA) traces of poly(methyl methacrylate) (PMMA) with various ω -chain ends derived from reversible addition-fragmentation chain transfer (RAFT) polymerization. (B) The extent of depolymerization of PMMA to methyl methacrylate (MMA) monomer as a function of ω -end-group identity, as determined by the extent of depolymerization prior to the plateaus in which no further mass loss is observed. Depolymerization experiments were performed in triplicate. Structures of studied RAFT agents are detailed in Figure 1B.

(Table S1). Unlike the other ATRP-derived polymers, depolymerization can be primarily attributed to thermolysis stemming from decarboxylation of the Phth ester and subsequent loss of isobutylene from the α -chain end of PMMA (Figures 1A and 3).

Given the successful depolymerization attributed to the Phth and TTC end-groups, we prepared a Phth-functional RAFT agent to access polymers that contained thermally labile moieties on both chain ends. We reasoned that more efficient depolymerization may be enabled by the higher concentration of thermally sensitive end-groups. A thiocarbonylthio compound (i.e., 1,3-dioxoisoindolin-2-yl 2-(((dodecylthio)carbonothioyl)thio)-2-methylpropanoate) (Phth-TTC) was prepared by esterifying 2-(dodecylthiocarbonothioylthio)-2-methylpropionic acid (DDMAT) with N-hydroxyphthalimide (Figures S6 and S7). The resulting Phth-TTC was subsequently used to polymerize MMA via photoiniferter polymerization, a polymerization method that enables high retention of the thiocarbonylthio moiety during polymerization to produce (Phth-PMMA-TTC, 5.4 kg/mol, Đ = 1.13) (Figure 4A). 57-63 Interestingly, unlike the trithiocarbonate precursor in which the R-group is generally not ideal for polymerization of methacrylate monomers (i.e., resulting in high dispersities and poor molecular weight control), the Phth-TTC provided a well-controlled polymerization (Figure S8). We attribute this to the electron-withdrawing nature of the Phth moiety facilitating more efficient β-cleavage of the R-group. 33,64 Gratifyingly, the combination of both chain ends in Phth-PMMA-TTC resulted in a much higher final extent of depolymerization (92%) compared with 42% for PMMA-TTC or 65% for Phth-PMMA-Br (Table S1). These data suggest that polymers capable of α - and ω -initiated depolymerization offer a promising route toward enhancing the efficiency of bulk depolymerizations.

We then examined the effect of molecular weight on the final extent of depolymerization (Figures 4A and 4B; Table S1). PMMA-TTC, Phth-PMMA, and Phth-PMMA-TTC polymers were prepared, ranging in molecular weight from 5.0 to 980 kg/mol. All of the polymers were subjected to a ramp rate of 10°C/min over a temperature range of 20°C–500°C. The extent of depolymerization was calculated by TGA as the mass loss observed up to the plateau region prior to the degradation temperature at 376°C. In addition to this method, the extent of depolymerization could also be calculated by subjecting polymer samples to an isothermal hold at 220°C for 2 h





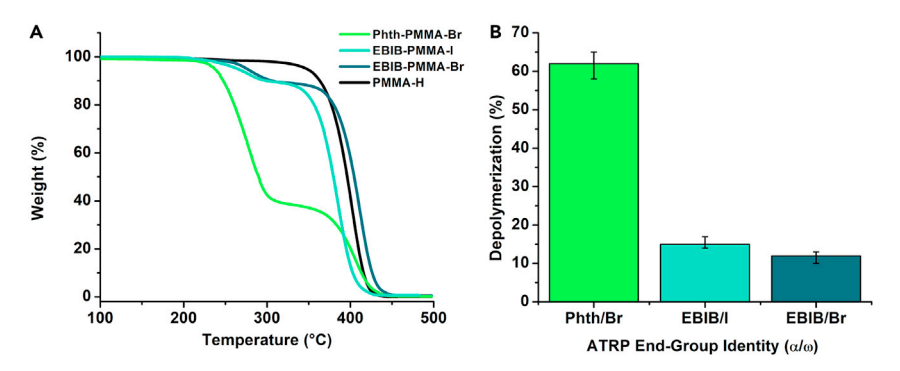


Figure 3. Extent of PMMA depolymerization utilizing ATRP end-groups

(A) Thermogravimetric analysis traces of poly(methyl methacrylate) (PMMA) with various α/ω -chain ends derived from atom-transfer radical polymerization (ATRP).

(B) The extent of depolymerization of PMMA to methyl methacrylate (MMA) monomer as a function of end-group identity, as determined by the extent of depolymerization prior to the plateaus in which no further mass loss is observed. Depolymerization experiments were performed in triplicate. Structures of the studied ATRP initiators are detailed in Figure 1C.

(Figure S9). The values determined by these two methods differed by less than 4%. The extent of depolymerization for low molecular weight PMMA-TTC reached up to 43%; however, polymer samples with higher molecular weights near 100 kg/mol achieved only 20% depolymerization. The Phth-PMMA polymers exhibited a similar trend in which low molecular weight polymers could achieve up to 65% depolymerization, but higher molecular weight polymers approaching 100 kg/mol achieved only 48% depolymerization. As mentioned previously, the combination of both chain ends in Phth-PMMA-TTC polymers resulted in the highest degrees of depolymerization. The Phth-PMMA-TTC polymers demonstrated a similar trend in which low molecular weight polymers could achieve up to 92% depolymerization, but higher molecular weight polymers approaching 100 kg/mol achieved only 62% depolymerization. To further probe the limitations of depolymerizing high molecular weight polymers, we employed photoiniferter polymerization to achieve ultrahigh molecular weight (UHMW) polymers, a class of materials that have garnered particular recent interest. 65-67 As such, a 980 kg/mol Phth-PMMA-TTC was synthesized, and 41% depolymerization was observed. These results suggest that the extent of depolymerization decreases with molecular weight, which is consistent with the results from depolymerizing under highly dilute conditions (Figure S9).⁶⁸

TGA analysis of the difunctional polymer indicated there were two separate onsets of depolymerization, the first at 150°C attributed to initiation from the ω -end TTC and the second at 220°C from the α -end Phth (Figure 5A; Table S1). Evidence for two separate mechanisms of chain-end-initiated depolymerization was further supported by the results of two separate, parallel isothermal holds, one at 180°C and the other 290°C for 20 min each. Analysis of the quantity of depolymerization via size-exclusion chromatography (SEC) indicated a mass loss of roughly 40%, which we attribute to depolymerization from the ω -end initiated by C–S thermolysis (Figure 5B, orange trace). The isothermal hold at 290°C resulted in 92% mass loss, 40% attributed to depolymerization from the ω -end TTC and an additional 52%, which we attribute to depolymerization induced by cleavage of the α -end Phth group (Figure 5B, blue trace). The final polymer byproduct was observed as a polymer of the same molecular weight as the starting polymer (Figure 5B, gray trace and S10). All methods in the determination of the extent of depolymerization were in good agreement and differed no more than 5% between SEC analysis, TGA analysis, and ¹H NMR analysis (Figure S11).





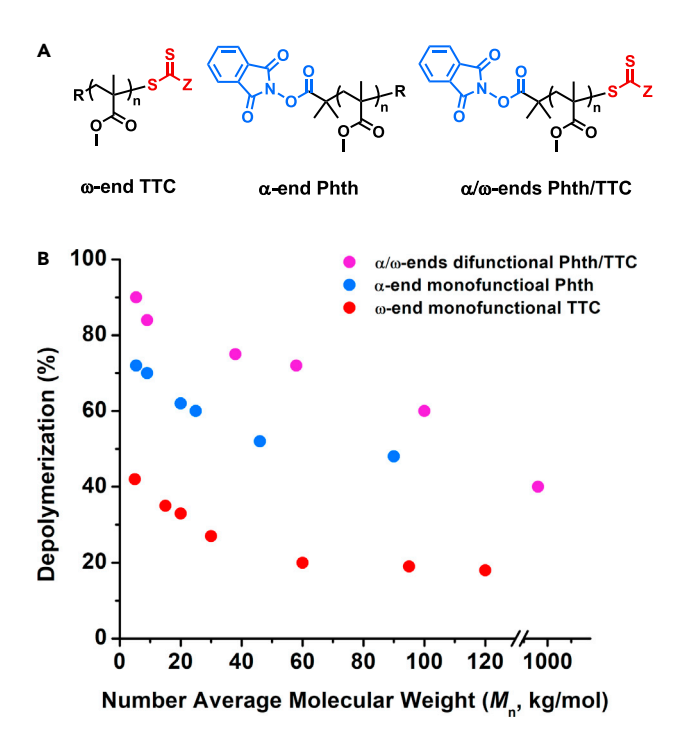


Figure 4. Depolymerization dependence on molecular weight

(A) Structures of PMMA with various α/ω end-groups.

(B) Examination of the dependence of the percent depolymerization on molecular weight (M_n) for ω (red), α (blue), and α/ω (purple) functionalized PMMA. PMMA of various molecular weights and endgroups were analyzed by TGA in which a heating rate of 10°C/min over a range of 20°C–500°C was used. The extent of depolymerization was determined by the percent mass loss up until the observed plateau prior to the degradation temperature of 376°C.

TGA-tandem mass spectrometry (TGA-MS) provided valuable insight into the mechanism of chain-end-initiated depolymerization by allowing analysis of the products liberated during thermal treatment (Figure 5C). Most importantly, throughout depolymerization the major product observed corresponded to that of the isotopes of MMA monomer (Figure 5C; Table S2). The generated byproducts helped to confirm our hypothesis that two separate onsets of depolymerization occur for the difunctional Phth-PMMA-TTC. For example, when Phth-PMMA-TTC was heated from 20°C to 500°C at a rate of 10°C/min, an ion fragment at 76 g/mol, indicating the release of CS₂, was detected at 170°C. This result suggests that higher temperatures near 170°C promote C-S homolysis to a PMMA radical, which readily depolymerizes and a TTC radical adduct that degrades to CS₂ and dodecane thiol.^{69,70} Furthermore, at 244°C ion fragments of 162 g/mol (Phth) were observed, which suggests cleavage from the α -chain end. A subsequent increase in MMA generation was observed indicating a second onset of depolymerization. From previous work, we hypothesize that the Phth group undergoes a decarboxylative degradation pathway with subsequent release of an isobutylene unit to generate a tertiary methacroyl radical capable of initiating depolymerization (Figure 1). Tracking ion fragments corresponding to CO₂ showed an increase in intensity at the second onset of depolymerization, corresponding to decarboxylation of the Phth ester (Figure S12). During both onsets of depolymerization, no MMA byproduct or dimer was observed. By contrast, unfunctionalized PMMA-H was found to require significantly higher temperatures to induce depolymerization (>376°C) as determined by TGA-MS. Degrading PMMA-H at 400°C led to ion fragments that correspond to MMA, but numerous byproducts were also present (Figure S13; Table S2). A significant mass peak at 102





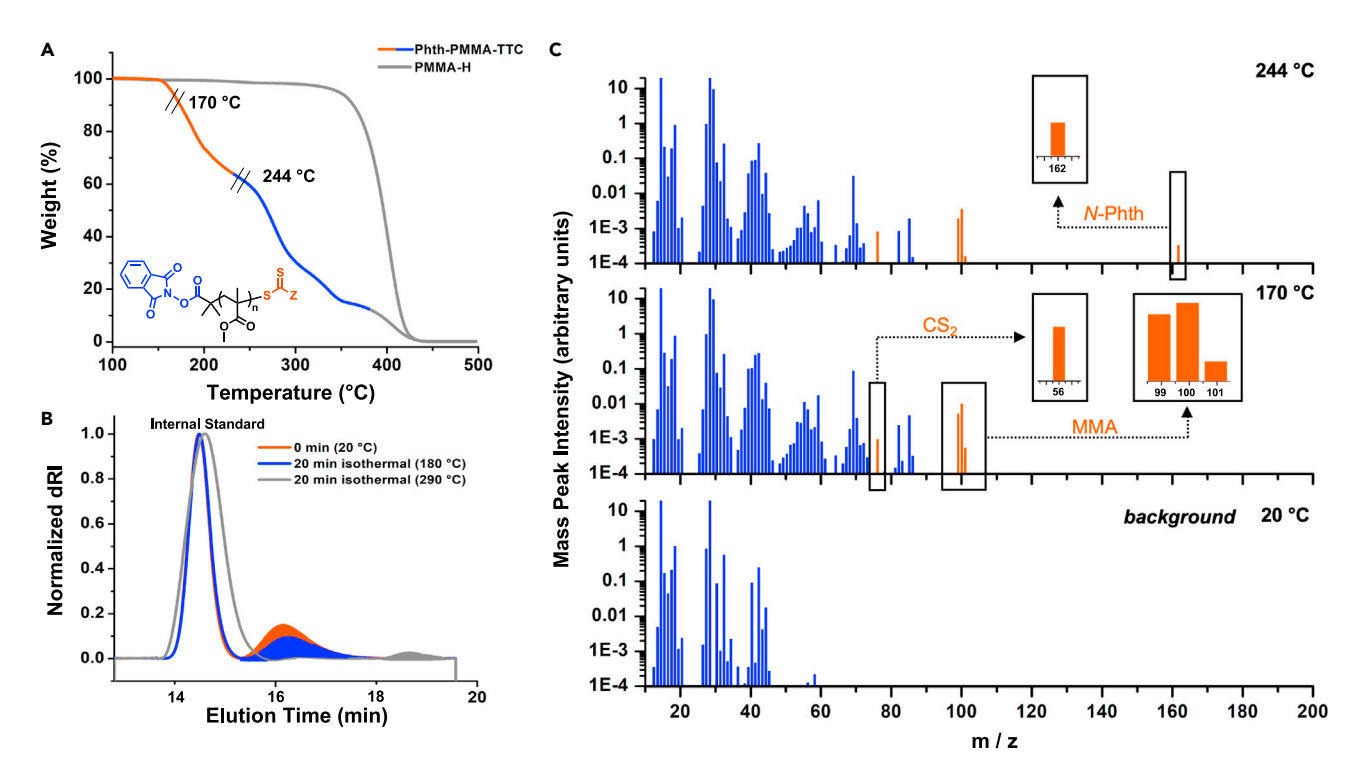


Figure 5. Depolymerization of PMMA utilizing telechelic end-groups for reversion to monomer

- $(A)\ Thermogravimetric\ analysis\ (TGA)\ of\ diffunctional\ Phth-PMMA-TTC\ with\ hashmarks\ representing\ the\ corresponding\ scans\ in\ (C).$
- (B) Size-exclusion chromatography traces of a 5.4 kg/mol difunctional Phth-PMMA-TTC relative to a 298 kg/mol polystyrene standard after two parallel isothermal holds at 180°C and 290°C .

(C) TGA-tandem mass spectrometry scans of a 5.4 kg/mol difunctional Phth-PMMA-TTC with key masses highlighted in orange. Ion fragment masses are detailed in Table S2.

g/mol corresponding to methyl pyruvate was observed, indicating that depolymerization initiated at higher temperatures generates undesired byproducts. Other masses at 90–99, 102–114, and 126 g/mol were also observed as distinct byproducts that were not present in TGA-MS spectra for functionalized PMMA samples (Table S2). Similar results have been shown by Marcantoni et al. in which unfunctionalized PMMA was degraded to monomer and as many as six other contaminant byproducts. ²⁴ These six contaminant byproducts were not detected via ¹H NMR analysis of the recovered monomer from PMMA-TTC, Phth-PMMA, or Phth-PMMA-TTC samples.

To demonstrate the viability of this PMMA depolymerization methodology for monomer recovery, we explored the bulk depolymerization of gram-scale quantities of PMMA-TTC (5.5 kg/mol), Phth-PMMA-Br (50 kg/mol), and Phth-PMMA-TTC (5.4 kg/mol) (Figure 6A). The bulk polymers were heated to 210°C–220°C and held for 1 h under vacuum to maximize monomer recovery (Figure 6B). Theoretical yields were determined by comparing the mass of the recovered monomer with the maximum mass loss during depolymerization observed by TGA. As expected, the monofunctional PMMA-TTC yielded the lowest reversion to monomer (43% mass loss, 94% theoretical yield, 0.35 mL MMA recovered). In comparison, Phth-PMMA-Br demonstrated modest monomer recovery (62% mass loss, 87% theoretical yield, 0.48 mL MMA recovered) (Figure 6C). Lastly, the difunctional Phth-PMMA-TTC yielded the highest reversion to monomer (92% mass loss, 88% theoretical yield, 0.93 mL MMA recovered). The remaining polymer products also





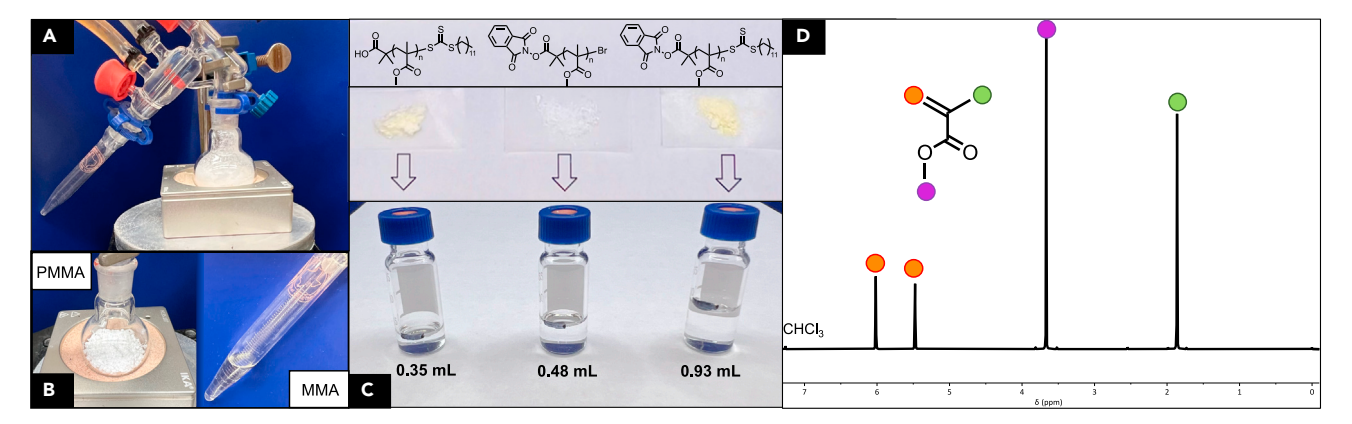


Figure 6. Bulk depolymerization of PMMA to MMA

- (A) Bulk depolymerization setup of PMMA to MMA.
- (B) Image of the bulk polymer and the recovered MMA.
- (C) Synthesized PMMA bearing different end-groups with quantity of monomer recovered after bulk depolymerization.
- (D) ¹H NMR spectrum of the recovered MMA.

contained byproducts from end-group degradation, such as Phth products and dodecanethiol, indicating that thermolytically active chain ends underwent thermolysis to initiate depolymerization but were not distilled with the generated MMA (Figure \$14). Terminal alkene peaks were observed in the Phth-PMMA and Phth-PMMA-TTC byproducts, in addition to the PMMA-TTC Chugaev-elimination product, suggesting that disproportionation occurs on the α -end as well (Figures S14-S16). Regardless, the resulting monomer from all bulk depolymerizations had high degrees of purity (Figures 6D, S18, and S19). In all three cases, monomer could be repolymerized to polymer without further purification (Figure S20). Although the telechelic Phth-PMMA-TTC material exhibited the highest monomer recovery, it is important to note that the Phth-PMMA may have the broadest utility because the material is colorless and transparent (Figure 6C). Solvent-cast films of the low molecular weight Phth-PMMA also demonstrated a high degree of transparency and lack of color relative to the TTC-containing materials (Figure S21), suggesting that these polymers may be useful for applications where colorless materials are desired. Furthermore, differential scanning calorimetry (DSC) analysis showed that the endfunctional polymers had similar glass transition temperatures (T_{α} s) to that of unfunctionalized PMMA (Figure S22).

The shape and breadth of polymer molecular weight distributions (MWDs) have significant influence on material properties of the polymers, such as processability and mechanical strength. 71,72 Although many recent reports have focused on tailoring initiation or using flow-mediated strategies to tune the MWD, the most widely used method to achieve different MWDs is through the physical blending of different polymers. $^{72-77}$ We hypothesized that by blending polymers with activatable chain ends (Phth-PMMA-TTC) and those without activatable chain ends (PMMA-H), the MWD could be further tuned through selective depolymerization. MWD tuning was achieved through the skew customization by unzipping layered polymer traces (SCULPT) method. As such, we examined how a set of three different polymers could be used to selectively skew the number-average molecular weight (M_n) toward a lower M_n , higher M_n , and inward toward a central M_n distribution. Two difunctional polymers (Phth-PMMA-TTC, 5.4 kg/mol, D = 1.13, 19.8 kg/mol, D = 1.30) were blended with an unfunctionalized polymer (PMMA-H, 12.0 kg/mol, D = 1.01) in various quantities to achieve mixed polymer distributions (Figure 7). Time points





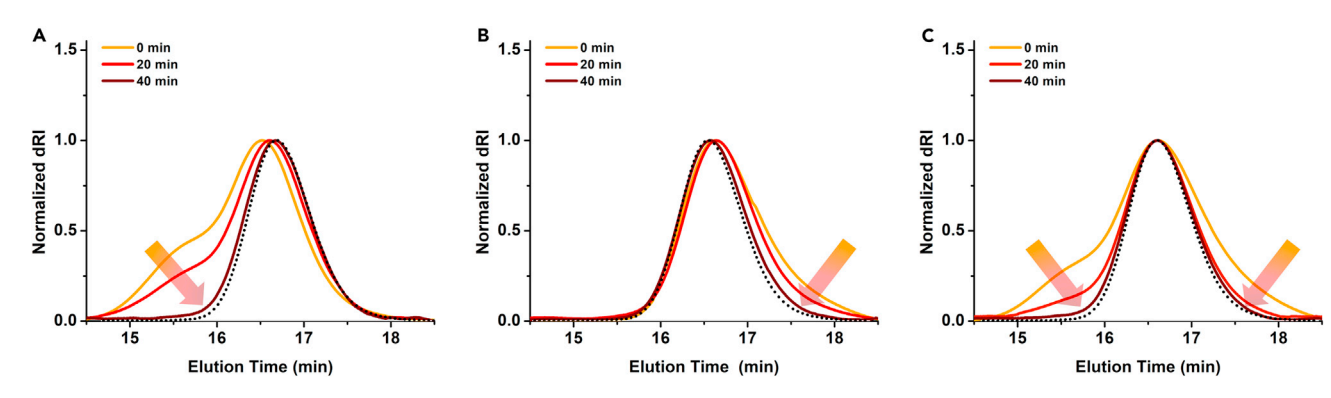


Figure 7. SCULPT depolymerization to monomodal polymer distributions

Size-exclusion chromatography (SEC) traces displaying the ability to depolymerize (A) blends with high molecular weight shoulders, (B) blends with low molecular weight shoulders, and (C) both high and low molecular weight shoulders from polymer blends, through their activatable chain ends with time. The unfunctionalized PMMA-H (12.0 kg/mol, D = 1.01) polymer trace is represented as a dotted line as a reference to the final molecular weight distributions achieved via the skew customization by unzipping layered polymer traces (SCULPT) method.

were taken at 0, 20, and 40 min to observe the suppression of the polymer trace associated with Phth-PMMA-TTC by SEC. In examining the ability to skew toward a low M_n distribution, a 1:1 weight mixture of functionalized Phth-PMMA-TTC (19.8 kg/mol, θ = 1.30) and unfunctionalized PMMA-H (12.0 kg/mol, θ = 1.01) was prepared to yield a final polymer blend with a broadened MWD (14.7, kg/mol, Đ = 1.18). An isothermal hold of the polymer blend at 290°C resulted in depolymerization of the Phth-PMMA-TTC to yield a final monomodal polymer distribution (11.8, kg/mol, θ = 1.05) that closely resembled that of the initial PMMA-H trace (Figure 7A). To analyze the possibility to skew toward a higher $M_{\rm n}$, a 1:1 weight mixture of the Phth-PMMA-TTC (5.4 kg/mol, D = 1.13) and PMMA-H (12 kg/mol, Đ = 1.01) was prepared yielding a final polymer blend with a broadened MWD (7.34 kg/mol, Đ = 1.32). In this case, an isothermal hold at 290°C resulted in nearquantitative disappearance of the low M_n difunctional Phth-PMMA-TTC to yield a final monomodal polymer distribution with a higher M_n (11.1 kg/mol, Θ = 1.06) (Figure 7B). Finally, to demonstrate the ability to skew toward a central M_n distribution through the SCULPT method, a blend containing 1:1:1 of both difunctional (5.5 kg/mol, D = 1.13 and 19.8 kg/mol, D = 1.30) and the unfunctionalizedPMMA-H (12 kg/mol, θ = 1.01) was prepared yielding a final polymer blend with a broadened MWD (8.3 kg/mol, Θ = 1.46). A final narrowed monomodal distribution (11.3 kg/mol, θ = 1.07) was achieved after an isothermal hold at 290°C, demonstrating the viability to selectively depolymerize both high- and low-molecular-weight chains while retaining a pre-determined, unfunctionalized central distribution (Figure 7C). In all three instances, depolymerization of the functionalized peak shoulders yielded nearly identical polymer traces to that of the unfunctionalized PMMA-H. We envision the SCULPT process to serve as a methodology to tune MWD for targeted material properties in future work.

Conclusions

The use of thermally labile chain ends for the bulk depolymerization of PMMA could facilitate the translation of PMMA synthesized by RDRP methods to industry by closing the life cycle circularity of polymeric materials. Our work demonstrates that RDRP-generated polymers are capable of undergoing thermally initiated depropagation at onset temperatures significantly lower than unfunctionalized PMMA. The ω -end trithiocarbonate and α -end Phth polymers resulted in the greatest extent of depolymerization at 42% and 65%, respectively. By utilizing a difunctional

Please cite this article in press as: Young et al., Bulk depolymerization of poly(methyl methacrylate) via chain-end initiation for catalyst-free reversion to monomer, Chem (2023), https://doi.org/10.1016/j.chempr.2023.07.004





photoiniferter, we installed both the trithiocarbonate and Phth chain ends on PMMA to achieve even higher degrees of depolymerization of 92%. Both end-groups facilitated reversion to monomer on the gram scale at 190°C–250°C lower than that required for unfunctionalized PMMA. We then examined the effect of molecular weight on the final extent of depolymerization and showed that even UHMW difunctional PMMA can achieve up to 41% depolymerization, setting a precedent for the ability to depolymerize a vast array of molecular weights. TGA-MS enabled observation of the ion fragments that correspond to the byproducts of chain-end cleavage, offering insight into mechanisms involving chain-end-initiated depolymerization. Furthermore, high-purity monomer was recovered and repolymerized without further purification. Lastly, our SCULPT process demonstrates that blended polymers can be selectively depolymerized to skew MWD, providing promise for end-of-life tuning of physical properties and monomer recovery in mixed polymer systems.

EXPERIMENTAL PROCEDURES

Resource availability

Lead contact

Further information and requests for resources should be directed to and will be fulfilled by the lead contact, Brent S. Sumerlin (sumerlin@chem.ufl.edu).

Materials availability

All materials generated in this study are available from the lead contact without restriction.

Data and code availability

All materials generated in this study are available from the lead contact without restriction.

SUPPLEMENTAL INFORMATION

Supplemental information can be found online at https://doi.org/10.1016/j.chempr. 2023.07.004.

ACKNOWLEDGMENTS

This material is based upon work supported by the National Science Foundation (DMR-1904631 and EEC-1941529) and the DoD through the ARO (W911NF-17-1-0326).

AUTHOR CONTRIBUTIONS

Conceptualization, J.B.Y., R.W.H., K.A.S., and B.S.S.; methodology, J.B.Y., R.W.H., and B.S.S.; validation, L.S.B.; formal analysis, J.B.Y. and R.W.H.; investigation, J.B.Y., R.W.H., A.M.T., and K.A.S.; data curation, J.B.Y. and R.W.H.; writing, J.B.Y., R.W.H., A.M.T., and B.S.S.; visualization, J.B.Y., R.W.H., L.S.B., and B.S.S.; supervision, B.S.S.; project administration, B.S.S.; funding acquisition, B.S.S.

DECLARATION OF INTERESTS

B.S.S. is a member of the Advisory Board for Chem.

INCLUSION AND DIVERSITY

One or more of the authors of this paper self-identifies as an underrepresented ethnic minority in their field of research or within their geographical location. One or more of the authors of this paper self-identifies as a gender minority in their field





of research. One or more of the authors of this paper self-identifies as a member of the LGBTQIA+ community. While citing references scientifically relevant for this work, we also actively worked to promote gender balance in our reference list.

Received: May 16, 2023 Revised: June 22, 2023 Accepted: July 11, 2023 Published: August 7, 2023

REFERENCES

- Schyns, Z.O.G., and Shaver, M.P. (2021). Mechanical recycling of packaging plastics: a review. Macromol. Rapid Commun. 42, e2000415. https://doi.org/10.1002/marc. 202000415.
- Rahimi, A.R., and Garciá, J.M. (2017). Chemical recycling of waste plastics for new materials production. Nat. Rev. Chem. 1, 1–11. https:// doi.org/10.1038/s41570-017-0046.
- Kim, D., Hinton, Z.R., Bai, P., Korley, L.T.J., Epps, T.H., and Lobo, R.F. (2022). Metathesis, molecular redistribution of alkanes, and the chemical upgrading of low-density polyethylene. Appl. Catal. B 318, 121873. https://doi.org/10.1016/j.apcatb.2022.121873.
- Saxon, D.J., Luke, A.M., Sajjad, H., Tolman, W.B., and Reineke, T.M. (2020). Nextgeneration polymers: isosorbide as a renewable alternative. Prog. Polym. Sci. 101, 101196. https://doi.org/10.1016/j. progpolymsci.2019.101196.
- Ragaert, K., Delva, L., and Van Geem, K. (2017). Mechanical and chemical recycling of solid plastic waste. Waste Manag. 69, 24–58. https:// doi.org/10.1016/j.wasman.2017.07.044.
- Hinton, Z.R., Talley, M.R., Kots, P.A., Le, A.V., Zhang, T., MacKay, M.E., Kunjapur, A.M., Bai, P., Vlachos, D.G., Watson, M.P., et al. (2022). Innovations toward the valorization of plastics waste. Annu. Rev. Mater. Res. 52, 249–280. https://doi.org/10.1146/annurev-matsci-081320-032344.
- Worch, J.C., and Dove, A.P. (2020). 100th Anniversary of Macromolecular Science Viewpoint: toward catalytic chemical recycling of waste (and Future) plastics. ACS Macro Lett. 9, 1494–1506. https://doi.org/10.1021/ acsmacrolett.0c00582.
- Jehanno, C., Pérez-Madrigal, M.M., Demarteau, J., Sardon, H., and Dove, A.P. (2019). Organocatalysis for depolymerisation. Polym. Chem. 10, 172–186. https://doi.org/10. 1039/C8PY01284A.
- Jehanno, C., Alty, J.W., Roosen, M., De Meester, S., Dove, A.P., Chen, E.Y.X., Leibfarth, F.A., and Sardon, H. (2022). Critical advances and future opportunities in upcycling commodity polymers. Nature 603, 803–814. https://doi.org/10.1038/s41586-021-04350-0.
- Shieh, P., Zhang, W., Husted, K.E.L., Kristufek, S.L., Xiong, B., Lundberg, D.J., Lem, J., Veysset, D., Sun, Y., Nelson, K.A., et al. (2020). Cleavable comonomers enable degradable, recyclable thermoset plastics. Nature 583, 542–547. https://doi.org/10.1038/s41586-020-2495-2.

- Kamiki, R., Kubo, T., and Satoh, K. (2023). Addition-fragmentation ring-opening polymerization of bio-based thiocarbonyl I-lactide for dual degradable vinyl copolymers. Macromol. Rapid Commun. 44, e2200537. https://doi.org/10.1002/marc.202200537.
- Wang, W., Zhou, Z., Sathe, D., Tang, X., Moran, S., Jin, J., Haeffner, F., Wang, J., and Niu, J. (2022). Degradable vinyl random copolymers via photocontrolled radical ring-opening cascade copolymerization**. Angew. Chem. Int. Ed. 134, 1–9. https://doi.org/10.1002/ange. 202113302.
- Huang, B., Wei, M., Vargo, E., Qian, Y., Xu, T., and Toste, F.D. (2021). Backbonephotodegradable polymers by incorporating acylsilane monomers via ring-opening metathesis polymerization. J. Am. Chem. Soc. 143, 17920–17925. https://doi.org/10.1021/ jacs.1c06836.
- Hill, M.R., Guégain, E., Tran, J., Figg, C.A., Turner, A.C., Nicolas, J., and Sumerlin, B.S. (2017). Radical ring-opening copolymerization of cyclic ketene acetals and maleimides affords homogeneous incorporation of degradable units. ACS Macro Lett. 6, 1071–1077. https:// doi.org/10.1021/acsmacrolett.7b00572.
- Smith, R.A., Fu, G., McAteer, O., Xu, M., and Gutekunst, W.R. (2019). Radical approach to thioester-containing polymers. J. Am. Chem. Soc. 141, 1446–1451. https://doi.org/10.1021/ jacs.8b12154.
- Spick, M.P., Bingham, N.M., Li, Y., De Jesus, J., Costa, C., Bailey, M.J., and Roth, P.J. (2020). Fully degradable thioester-functional homoand alternating copolymers prepared through thiocarbonyl addition-ring-opening RAFT radical polymerization. Macromolecules 53, 539–547. https://doi.org/10.1021/acs. macromol.9b02497.
- Kimura, T., Kuroda, K., Kubota, H., and Ouchi, M. (2021). Metal-catalyzed switching degradation of vinyl polymers via introduction of an "in-chain" carbon-halogen bond as the trigger. ACS Macro Lett. 10, 1535–1539. https://doi.org/10.1021/acsmacrolett.1c00601.
- Makino, H., Nishikawa, T., and Ouchi, M. (2022). Incorporation of a boryl pendant as the trigger in a methacrylate polymer for backbone degradation. Chem. Commun. (Camb) 58, 11957–11960. https://doi.org/10.1039/ d2cc04882e.
- Adili, A., Korpusik, A.B., Seidel, D., and Sumerlin, B.S. (2022). Photocatalytic direct decarboxylation of carboxylic acids to derivatize or degrade polymers. Angew.

- Chem. Int. Ed. Engl. 61, e202209085. https://doi.org/10.1002/anie.202209085.
- Garrison, J.B., Hughes, R.W., and Sumerlin, B.S. (2022). Backbone degradation of polymethacrylates via metal-free ambienttemperature photoinduced single-electron transfer. ACS Macro Lett. 11, 441–446. https:// doi.org/10.1021/acsmacrolett.2c00091.
- Garrison, J.B., Hughes, R.W., Young, J.B., and Sumerlin, B.S. (2022). Photoinduced SET to access olefin-acrylate copolymers. Polym. Chem. 13, 982–988. https://doi.org/10.1039/ D1PY01643A.
- Neary, W.J., Isais, T.A., and Kennemur, J.G. (2019). Depolymerization of bottlebrush Polypentenamers and their macromolecular metamorphosis. J. Am. Chem. Soc. 141, 14220– 14229. https://doi.org/10.1021/jacs.9b05560.
- De Tommaso, J., and Dubois, J.L. (2021). Risk analysis on PMMA recycling economics. Polymers (Basel) 13, 2724. https://doi.org/10. 3390/polym13162724.
- Godiya, C.B., Gabrielli, S., Materazzi, S., Pianesi, M.S., Stefanini, N., and Marcantoni, E. (2019). Depolymerization of waste poly(methyl methacrylate) scraps and purification of depolymerized products. J. Environ. Manage. 231, 1012–1020. https://doi.org/10.1016/j. jenvman.2018.10.116.
- Matyjaszewski, K., and J.X. (2001). Atom transfer radical polymerization. Chem. Rev. 101, 2921–2990. https://doi.org/10.1002/ 9783527809080.cataz01278.
- Matyjaszewski, K. (2012). Atom transfer radical polymerization (ATRP): current status and future perspectives. Macromolecules 45, 4015– 4039. https://doi.org/10.1021/ma3001719.
- Dadashi-Silab, S., and Matyjaszewski, K. (2020). Iron catalysts in atom transfer radical polymerization. Molecules 25, 1648. https:// doi.org/10.3390/molecules25071648.
- Horn, M., and Matyjaszewski, K. (2013). Solvent effects on the activation rate constant in atom transfer radical polymerization. Macromolecules 46, 3350–3357. https://doi. org/10.1021/ma400565k.
- Hill, M.R., Carmean, R.N., and Sumerlin, B.S. (2015). Expanding the scope of RAFT polymerization: recent advances and new horizons. Macromolecules 48, 5459–5469. https://doi.org/10.1021/acs.macromol. 5b00342.
- 30. Keddie, D.J., Moad, G., Rizzardo, E., and Thang, S.H. (2012). RAFT agent design and





- synthesis. Macromolecules 45, 5321–5342. https://doi.org/10.1021/ma300410v.
- Moad, G., Rizzardo, E., and Thang, S.H. (2009). Living radical polymerization by the RAFT process A second update. Aust. J. Chem. 62, 1402–1472. https://doi.org/10.1071/CH09311.
- 32. Moad, G., Chiefari, J., Chong, Y.K., Krstina, J., Mayadunne, R.T., Postma, A., Rizzardo, E., and Thang, S.H. (2000). Living free radical polymerization with reversible addition-fragmentation chain transfer (the life of RAFT). Polym. Int. 49, 993–1001. https://doi.org/10.1002/1097-0126(200009)49:9<993::AID-PI506>3.0.CO;2-6.
- Perrier, S. (2017). 50th Anniversary Perspective: RAFT Polymerization - A User Guide. Macromolecules 50, 7433–7447. https://doi. org/10.1021/acs.macromol.7b00767.
- Haddleton, D.M., Jasieczek, C.B., Hannon, M.J., and Shooter, A.J. (1997). Atom transfer radical polymerization of methyl methacrylate initiated by alkyl bromide and 2-pyridinecarbaldehyde imine copper(I) Complexes. Macromolecules 30, 2190–2193. https://doi.org/10.1021/ma961074r.
- Lessard, J.J., Scheutz, G.M., Hughes, R.W., and Sumerlin, B.S. (2020). Polystyrene-based vitrimers: inexpensive and recyclable thermosets. ACS Appl. Polym. Mater. 2, 3044– 3048. https://doi.org/10.1021/acsapm. 0r00523
- Flanders, M.J., and Gramlich, W.M. (2018). Reversible-addition fragmentation chain transfer (RAFT) mediated depolymerization of brush polymers. Polym. Chem. 9, 2328–2335. https://doi.org/10.1039/C8PY00446C.
- Sano, Y., Konishi, T., Sawamoto, M., and Ouchi, M. (2019). Controlled radical depolymerization of chlorine-capped PMMA via reversible activation of the terminal group by ruthenium catalyst. Eur. Polym. J. 120, 109181. https://doi. org/10.1016/j.eurpolymj.2019.08.008.
- Wang, H.S., Truong, N.P., Pei, Z., Coote, M.L., and Anastasaki, A. (2022). Reversing RAFT polymerization: near-quantitative monomer generation via a catalyst-free depolymerization approach. J. Am. Chem. Soc. 144, 4678–4684. https://doi.org/10.1021/jacs.2c00963.
- Young, J.B., Bowman, J.I., Eades, C.B., Wong, A.J., and Sumerlin, B.S. (2022). Photoassisted radical depolymerization. ACS Macro Lett. 11, 1390–1395. https://doi.org/10.1021/ acsmacrolett.2c00603.
- Bellotti, V., Parkatzidis, K., Wang, H.S., De Alwis Watuthanthrige, N., Orfano, M., Monguzzi, A., Truong, N.P., Simonutti, R., and Anastasaki, A. (2023). Light-accelerated depolymerization catalyzed by eosin Y. Polym. Chem. 14, 253–258. https://doi.org/10.1039/d2py01383e.
- Martinez, M.R., Schild, D., De Luca Bossa, F., and Matyjaszewski, K. (2022). Depolymerization of polymethacrylates by iron ATRP. Macromolecules 55, 10590–10599. https://doi. org/10.1021/acs.macromol.2c01712.
- Martinez, M.R., De Luca Bossa, F., Olszewski, M., and Matyjaszewski, K. (2022). Copper(II) chloride/Tris(2-pyridylmethyl)amine-Catalyzed Depolymerization of poly(n-butyl methacrylate). Macromolecules 55, 78–87.

- https://doi.org/10.1021/acs.macromol. 1c02246.
- Martinez, M.R., Dadashi-Silab, S., Lorandi, F., Zhao, Y., and Matyjaszewski, K. (2021). Depolymerization of P(PDMS11MA) bottlebrushes via atom transfer radical polymerization with activator regeneration. Macromolecules 54, 5526–5538. https://doi. org/10.1021/acs.macromol.1c00415.
- 44. Wan, L.R., Ruiz, R., Gao, H., Patel, K.C., Albrecht, T.R., Yin, J., Kim, J., Cao, Y., and Lin, G. (2015). The limits of lamellae-forming PS-b-PMMA Block Copolymers for Lithography. ACS Nano 9, 7506–7514. https://doi.org/10.1021/ acsnano.5b02613.
- Snow, R.D., and Frey, F.E. (1943). The reaction of sulfur dioxide with olefins: the ceiling temperature phenomenon. J. Am. Chem. Soc. 65, 2417–2418. https://doi.org/10.1021/ ia01252a052.
- Dainton, F.S., and Ivin, K.J. (1948). Reversibility
 of the propagation reaction in polymerization
 processes and its manifestation in the
 phenomenon of a "ceiling temperature.".
 Nature 162, 705–707. https://doi.org/10.1038/
 162705a0.
- Postma, A., Davis, T.P., Moad, G., and O'Shea, M.S. (2005). Thermolysis of RAFT-synthesized polymers. A convenient method for trithiocarbonate group elimination. Macromolecules 38, 5371–5374. https://doi. org/10.1021/ma050402x.
- DePuy, C.H., and King, R.W. (1960). Pyrolitic cis eliminations. Chem. Rev. 60, 431–457. https:// doi.org/10.1021/cr60207a001.
- Perrier, S., and Takolpuckdee, P. (2005). Macromolecular design via reversible addition-fragmentation chain transfer (RAFT)/xanthates (MADIX) polymerization. J. Polym. Sci. A Polym. Chem. 43, 5347–5393. https://doi.org/10.1002/pola.20986.
- Chong, B., Moad, G., Rizzardo, E., Skidmore, M., and Thang, S.H. (2006). Thermolysis of RAFT-synthesized poly (methyl methacrylate). Aust. J. Chem. 59, 755–762.
- Bekanova, M.Z., Neumolotov, N.K., Jablanović, A.D., Plutalova, A.V., Chernikova, E.V., and Kudryavtsev, Y.V. (2019). Thermal stability of RAFT-based poly(methyl methacrylate): A kinetic study of the dithiobenzoate and trithiocarbonate end-group effect. Polym. Degrad. Stab. 164, 18–27. https://doi.org/10. 1016/j.polymdegradstab.2019.03.017.
- Whitfield, R., Anastasaki, A., Nikolaou, V., Jones, G.R., Engelis, N.G., Discekici, E.H., Fleischmann, C., Willenbacher, J., Hawker, C.J., and Haddleton, D.M. (2017). Universal conditions for the controlled polymerization of acrylates, methacrylates, and styrene via Cu(0)-RDRP. J. Am. Chem. Soc. 139, 1003–1010. https://doi.org/10.1021/jacs.6b11783.
- Konkolewicz, D., Schröder, K., Buback, J., Bernhard, S., and Matyjaszewski, K. (2012). Visible light and sunlight photoinduced ATRP with ppm of Cu catalyst. ACS Macro Lett. 1, 1219–1223. https://doi.org/10.1021/ pr.300457e.
- Szczepaniak, G., Jeong, J., Kapil, K., Dadashi-Silab, S., Yerneni, S.S., Ratajczyk, P., Lathwal, S., Schild, D.J., Das, S.R., and Matyjaszewski, K.

- (2022). Open-air green-light-driven ATRP enabled by dual photoredox/copper catalysis. Chem. Sci. 13, 11540–11550. https://doi.org/10.1039/d2sc04210j.
- Parkatzidis, K., Boner, S., Wang, H.S., and Anastasaki, A. (2022). Photoinduced ironcatalyzed ATRP of renewable monomers in low-toxicity solvents: A greener approach. ACS Macro Lett. 11, 841–846. https://doi.org/10. 1021/acsmacrolett.2c00302.
- Nguyen, N.H., Rosen, B.M., Lligadas, G., and Percec, V. (2009). Surface-Dependent kinetics of Cu(0)-Wire-Catalyzed single-electron transfer living radical polymerization of methyl acrylate in DMSO at 25 °C. Macromolecules 42, 2379–2386. https://doi.org/10.1021/ ma8028562.
- Hughes, R.W., Lott, M.E., Bowman, J.I., and Sumerlin, B.S. (2023). Excitation dependence in photoiniferter polymerization. ACS Macro Lett. 12, 14–19. https://doi.org/10.1021/ acsmacrolett.2c00683.
- Lee, Y., Boyer, C., and Kwon, M.S. (2023). Photocontrolled RAFT polymerization: past, present, and future. Chem. Soc. Rev. 52, 3035– 3097. https://doi.org/10.1039/d1cs00069a.
- Bagheri, A. (2023). Application of RAFT in 3D printing: where are the future opportunities? Macromolecules 56, 1778–1797. https://doi. org/10.1021/acs.macromol.2c02585.
- Hartlieb, M. (2022). Photo-iniferter RAFT polymerization. Macromol. Rapid Commun. 43, e2100514. https://doi.org/10.1002/marc. 202100514.
- Lehnen, A.-C., Gurke, J., Bapolisi, A.M., Reifarth, M., and Bekir, M. (2023). Xanthatesupported photo-iniferter (XPI)-RAFT polymerization: facile and rapid access to complex macromolecules. Chem. Sci. 14, 593–603. https://doi.org/10.4324/ 9781003117711-5.
- Lehnen, A.-C.C., Kurki, J.A.M.M., and Hartlieb, M. (2022). The difference between photoiniferter and conventional RAFT polymerization: high livingness enables the straightforward synthesis of multiblock copolymers. Polym. Chem. 13, 1537–1546. https://doi.org/10.1039/D1PY01530C.
- Zhou, H., and Johnson, J.A. (2013). Photocontrolled growth of telechelic polymers and end-linked polymer gels. Angew. Chem. Int. Ed. 125, 2291–2294. https://doi.org/10.1002/ ange.201207966.
- Easterling, C.P., Xia, Y., Zhao, J., Fanucci, G.E., and Sumerlin, B.S. (2019). Block copolymer sequence inversion through photoiniferter polymerization. ACS Macro Lett. 8, 1461–1466. https://doi.org/10.1021/acsmacrolett. 9b00716.
- Carmean, R.N., Becker, T.E., Sims, M.B., and Sumerlin, B.S. (2017). Ultra-high molecular weights via aqueous reversible-deactivation radical polymerization. Chem 2, 93–101. https://doi.org/10.1016/j.chempr.2016.12.007.
- Olson, R.A., Lott, M.E., Garrison, J.B., Davidson, C.L.G., Trachsel, L., Pedro, D.I., Sawyer, W.G., and Sumerlin, B.S. (2022). Inverse miniemulsion photoiniferter polymerization for the synthesis of ultra-high molecular weight polymers. Macromolecules 55, 8451–8460.

Please cite this article in press as: Young et al., Bulk depolymerization of poly(methyl methacrylate) via chain-end initiation for catalyst-free reversion to monomer, Chem (2023), https://doi.org/10.1016/j.chempr.2023.07.004





- https://doi.org/10.1021/acs.macromol. 2c01239.
- 67. Carmean, R.N., Sims, M.B., Figg, C.A., Hurst, P.J., Patterson, J.P., and Sumerlin, B.S. (2020). Ultrahigh molecular weight hydrophobic acrylic and Styrenic polymers through organicphase photoiniferter-mediated polymerization. ACS Macro Lett. 9, 613–618. https://doi.org/10.1021/acsmacrolett.0c00203.
- 68. Wang, H.S., Truong, N.P., Jones, G.R., and Anastasaki, A. (2022). Investigating the effect of end-group, molecular weight, and solvents on the catalyst-free depolymerization of RAFT polymers: possibility to reverse the polymerization of heat-sensitive polymers. ACS Macro Lett. 11, 1212–1216. https://doi.org/10. 1021/acsmacrolett.2c00506.
- Fu, Q., McKenzie, T.G., Tan, S., Nam, E., and Qiao, G.G. (2015). Tertiary amine catalyzed photo-induced controlled radical polymerization of methacrylates. Polym. Chem. 6, 5362–5368. https://doi.org/10.1039/ C5PY00840A.

- Fu, Q., Xie, K., McKenzie, T.G., and Qiao, G.G. (2017). Trithiocarbonates as intrinsic photoredox catalysts and RAFT agents for oxygen tolerant controlled radical polymerization. Polym. Chem. 8, 1519–1526. https://doi.org/10.1039/ C6PY01994C.
- Gentekos, D.T., Sifri, R.J., and Fors, B.P. (2019). Controlling polymer properties through the shape of the molecular-weight distribution. Nat. Rev. Mater. 4, 761–774. https://doi.org/10. 1038/s41578-019-0138-8.
- Whitfield, R., Truong, N.P., Messmer, D., Parkatzidis, K., Rolland, M., and Anastasaki, A. (2019). Tailoring polymer dispersity and shape of molecular weight distributions: methods and applications. Chem. Sci. 10, 8724–8734. https://doi.org/10.1039/c9sc03546j.
- Kottisch, V., Gentekos, D.T., and Fors, B.P. (2016). "Shaping" the Future of molecular weight Distributions in Anionic Polymerization. ACS Macro Lett. 5, 796–800. https://doi.org/10. 1021/acsmacrolett.6b00392.

- Whitfield, R., Truong, N.P., and Anastasaki, A. (2021). Precise control of both dispersity and molecular weight distribution shape by polymer blending. Angew. Chem. Int. Ed. 133, 19532–19537. https://doi.org/10.1002/ange. 202106729
- Corrigan, N., and Boyer, C. (2022). Living in the moment: A mathematically verified approach for molecular weight distribution analysis and application to data storage. Macromolecules 55, 8960–8969. https://doi.org/10.1021/acs. macromol.2c00945.
- Gentekos, D.T., and Fors, B.P. (2018). Molecular weight distribution shape as a versatile approach to tailoring block copolymer phase behavior. ACS Macro Lett. 7, 677–682. https://doi.org/10.1021/acsmacrolett. 8b00295.
- Rosenbloom, S.I., Sifri, R.J., and Fors, B.P. (2021). Achieving molecular weight distribution shape control and broad dispersities using RAFT polymerizations. Polym. Chem. 12, 4910– 4915. https://doi.org/10.1039/D1PY00399B.